Table XIII. Ligand Effects on the Oscillator Strengths of Hypersensitive Transitions

	f(complex)/*f*(aquo)			
complex	Nd(e)[a]	Ho(d)[b]	Er(c)[c]	Er(h)[d]
Ln(ODA)	1.29	2.79	2.08	1.88
Ln(MIDA)	1.60	3.03	2.75	2.49
Ln(IDA)	1.68	3.12	2.26	2.05
Ln(DPA)	2.00	3.86	2.95	2.65
Ln(CDA)	2.89	5.73	5.08	(4.15)[e]
Ln(CDO)	2.90	6.19	4.45	(3.58)[e]

[a] $^4I_{9/2} \rightarrow {}^4G_{5/2}, {}^2G_{7/2}$; absorption band centered near 580 nm. [b] $^5I_8 \rightarrow {}^5G_6, {}^5F_1$; absorption band centered near 450 nm. [c] $^4I_{15/2} \rightarrow {}^2H_{11/2}$; absorption band centered near 520 nm. [d] $^4I_{15/2} \rightarrow {}^4G_{11/2}$; absorption band centered near 380 nm. See ref 11. [e] Calculated from fitted oscillator strength data. See ref 11.

measured for these transitions. In addition to the *f*(complex)/*f*(aquo) ratios given in Table XIII, it is interesting to note the oscillator-strength ratios for Ln(ODA) vs Ln(DPA) vs Ln(CDA). The latter are approximately the same for the different transitions: 1.00 (ODA):1.45 (DPA):2.20 (CDA). Recall that the Ln(CDA) complexes differ from the Ln(DPA) complexes only by a 4-oxo substituent on the pyridyl ring of the central donor moiety of each ligand. However, this small difference produces a 50% increase in the intensities of the hypersensitive transitions.

The transitions making the major contributions to the hypersensitive absorption bands are as follows: $^4I_{9/2} \rightarrow {}^4G_{5/2}$, Nd(e); $^5I_8 \rightarrow {}^5G_6$, Ho(d); $^4I_{15/2} \rightarrow {}^2H_{11/2}$, Er(c); $^4I_{15/2} \rightarrow {}^4G_{11/2}$, Er(h). Each of these transitions nominally satisfies electric-quadrupole selection rules for ΔJ and ΔL, and the ΔS selection rule is also satisfied at least in part, since the $^2H_{11/2}$ and $^4G_{11/2}$ multiplets of Er^{3+} are strongly mixed in the intermediate-coupling scheme (see Table II of ref 11). According to our model calculations, the *electric-dipole* intensities of these transitions are derived primarily from correlated *dynamic couplings* between 4f–4f electric-quadrupolar transition densities and transient electric dipoles produced in polarizable ligand groups by the incident radiation field. The transition intensities depend on the strength (and symmetry) of the dynamic couplings, and the latter depend on the distribution, magnitude, and anisotropy of ligand polarizability.[13,14,17] The relative oscillator strengths listed in Table XIII for the Ln(ODA), Ln(DPA), Ln(CDA), and Ln(CDO) complexes do correlate with relative ligand polarizabilities. On the other hand, the relative oscillator strengths of the Ln(ODA), Ln(MIDA), and Ln(IDA) complexes probably reflect structural (geometrical) differences as well as differences in ligand polarizability.

The ligand-dependent intensity variations observed in the hypersensitive transitions examined in this study are quite satisfactorily accounted for by the dynamic-coupling mechanism in our intensity model. However, it is possible that other mechanisms, not included in our model, may also be important in producing these intensity variations. Recall that our model neglects all effects that might arise from f-orbital overlap with ligand orbitals (including covalency effects). It is likely that these effects will appear most prominently in the Ω_6 intensity parameters and least prominently in the Ω_2 parameters but definitive intensity calculations including orbital overlap effects have not yet been reported.

Acknowledgment. This work was supported by the National Science Foundation (NSF Grant CHE-8215815 to F.S.R.), by the National Institutes of Health (Grants DK35865 and SO7 RR05431-24 to E.M.S.), and by a grant from the Muscular Dystrophy Association (to E.M.S.).

Registry No. $Nd(ODA)_3^{3-}$, 43030-80-4; $Ho(ODA)_3^{3-}$, 58855-74-6; $Er(ODA)_3^{3-}$, 83289-78-5; $Nd(DPA)_3^{3-}$, 38721-35-6; $Ho(DPA)_3^{3-}$, 38785-79-4; $Er(DPA)_3^{3-}$, 38682-38-1; $Nd(CDO)_3^{6-}$, 113474-75-2; $Ho(CDO)_3^{6-}$, 113474-74-1; $Er(CDO)_3^{6-}$, 107454-34-2; $Nd(CDA)_3^{6-}$, 113474-77-4; $Ho(CDA)_3^{6-}$, 113474-76-3; $Er(CDA)_3^{6-}$, 107454-33-1; $Nd(IDA)_3^{3-}$, 12561-55-6; $Ho(IDA)_3^{3-}$, 83233-72-1; $Er(IDA)_3^{3-}$, 83289-79-6; $Nd(MIDA)_3^{3-}$, 89746-87-2; $Ho(MIDA)_3^{3-}$, 83233-73-2; $Er(MIDA)_3^{3-}$, 83248-18-4; $Nd(H_2O)_9^{3+}$, 54375-24-5; $Ho(H_2O)_9^{3+}$, 55664-37-4; $Er(H_2O)_9^{3+}$, 56422-25-4; $Nd(H_2O)_8^{3+}$, 62006-59-1; $Ho(H_2O)_8^{3+}$, 63213-08-1; $Er(H_2O)_8^{3+}$, 63118-71-8; Nd^{3+}, 14913-52-1; Ho^{3+}, 22541-22-6; Er^{3+}, 18472-30-5.

Contribution from the Department of Chemistry, University of Missouri—Rolla, Rolla, Missouri 65401, Department of Physics, University of Liverpool, Liverpool L69 3BX, England, Institut de Physique, Universite de Liège, B-4000 Sart-Tilman, Belgium, and Dipartimento di Chimica Inorganica, Metallorganica ed Analitica, Universita di Padova, Via Loredan, 4, I-35131 Padova, Italy

Mössbauer Effect Study of $Fe_3(CO)_{12}$

Fernande Grandjean, Gary J. Long,* Christopher G. Benson, and Umberto Russo

Received September 22, 1987

The Mössbauer effect spectrum of $Fe_3(CO)_{12}$ has been measured from 4.2 to 295 K, and the results, when analyzed in terms of the two expected quadrupole doublets, reveal an unusual temperature dependence, first in the quadrupole interaction for the unique nonbridged iron site, second in the relative area of the two components of the quadrupole doublet associated with the two chemically equivalent carbonyl-bridged iron sites, and third in the relative area of these two quadrupole doublets. The first of these may be understood in terms of a negative quadrupole interaction for the unique iron site, produced principally by a negative, temperature-dependent, valence contribution to the electric field gradient. The second results from the large vibrational anisotropy associated with the bridged iron sites, which leads to the Goldanskii–Karyagin effect and an asymmetric doublet. An analysis based on the single-crystal thermal ellipsoid anisotropy of the bridged iron sites is successful in explaining the observed asymmetry. The third results from the different temperature dependence of the recoil-free fractions observed for the two chemically quite dissimilar iron sites.

Introduction

The determination of the solid-state structure of triiron dodecacarbonyl, $Fe_3(CO)_{12}$ (I), a 50-year story, was nicely summarized by Desiderato and Dobson.[1] Its single-crystal structure was solved by Wei and Dahl[2] and further refined by Cotton and Troup.[3] The molecule has C_{2v} symmetry as shown in Figure 1 and has one unique iron atom, Fe_1 or Fe_A, bonded to four terminal

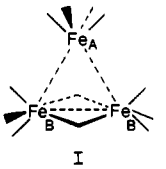

I

carbonyl ligands and two chemically equivalent iron atoms, Fe_2 and Fe_3 or Fe_B, bonded to three terminal carbonyl and two

* To whom correspondence should be addressed at the University of Missouri—Rolla.

(1) Desiderato, R., Jr.; Dobson, G. R. *J. Chem. Educ.* **1982**, *59*, 752–756.

0020-1669/88/1327-1524$01.50/0

Table I. Mössbauer Spectral Parameters for $Fe_3(CO)_{12}$

T, K	concn, mg/cm²	δ_A,[a] mm/s	$\Delta E_{Q,A}$, mm/s	Γ_A, mm/s	% area	δ_B,[a] mm/s	$\Delta E_{Q,B}$, mm/s	Γ_B, mm/s	A_1/A_4	% area	A_B/A_A	tot. area, (% ϵ) × (mm/s)
295	25	−0.012	−0.197	0.31	46	0.022	0.944	0.26	0.78	54	1.16	7.10
273		−0.001	−0.186	0.30	45	0.036	0.961	0.24	0.80	55	1.22	7.99
253		0.009	−0.176	0.30	44	0.048	0.987	0.24	0.84	56	1.28	11.07
189		0.047	−0.104	0.33	43	0.094	1.046	0.25	0.89	57	1.32	18.67
142		0.058	−0.087	0.34	41	0.109	1.072	0.26	0.92	59	1.45	23.5
78		0.078	−0.079	0.34	39	0.133	1.116	0.27	0.96	61	1.59	31.5
295	10	−0.008	−0.193	0.29	44	0.022	0.931	0.27	0.72	56	1.27	
189		0.045	−0.106	0.34	42	0.087	1.036	0.25	0.88	58	1.38	
78		0.076	−0.079	0.32	38	0.132	1.119	0.25	0.95	62	1.63	
4.2		0.074	−0.084	0.26	35	0.134	1.146	0.25	1.01	65	1.90	
295[b]	10	−0.011	−0.198	0.29	44	0.019	0.937	0.27	0.78	56	1.26	

[a] Relative to room-temperature natural α-iron foil. [b] Obtained from the sum of four spectra measured at the magic angle (see text).

bridging carbonyl ligands. As illustrated in Figure 1, the single-crystal structure shows two equivalent statistically disordered orientations of the iron triangle within the fixed framework of the twelve carbonyl ligands. These two triangle orientations form a Star of David like structure, II. The molecular structure, I,

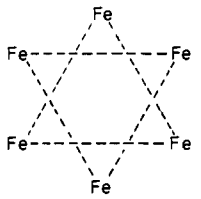

II

was first proposed virtually simultaneously, in 1965, by Erickson and Fairhall,[4] who based their proposal on Mössbauer spectral data, and by Dahl and Blount,[5] who based their proposal on Mössbauer and infrared data and structural data obtained for $[HFe_3(CO)_{11}]^-$ (III). The Mössbauer spectrum of $Fe_3(CO)_{12}$

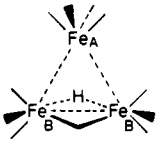

III

obtained[6] at 78 K reveals three lines of nearly equal intensity. The spectrum was analyzed[4,6] by superimposing a quadrupole doublet, with a splitting of 1.12 mm/s resulting from the two equivalent iron atoms, Fe_B, upon a singlet, resulting from the unique iron atom, Fe_A.

In this paper we present an extensive Mössbauer spectral study of $Fe_3(CO)_{12}$ (I) from 4.2 to 295 K. The surprising changes that occur with temperature, both in the spectral hyperfine parameters and in the relative line areas, indicate a negative quadrupole interaction on the Fe_A site, a distinct difference in the temperature dependence of the recoil-free fraction of the Fe_A and Fe_B sites, and a Goldanskii–Karyagin effect due to an anisotropic recoil-free fraction for the Fe_B sites.

Experimental Section

$Fe_3(CO)_{12}$ was obtained from BDH or Alfa Inorganics and was recrystallized from 50:50 acetone water just prior to use. A sample that was sublimed immediately prior to study gave an identical room-temperature Mössbauer spectrum. The Mössbauer effect spectra were obtained on a Harwell constant-acceleration spectrometer, which utilized a room-temperature rhodium matrix cobalt-57 source and was calibrated at room temperature with α-iron foil. The Mössbauer effect absorbers

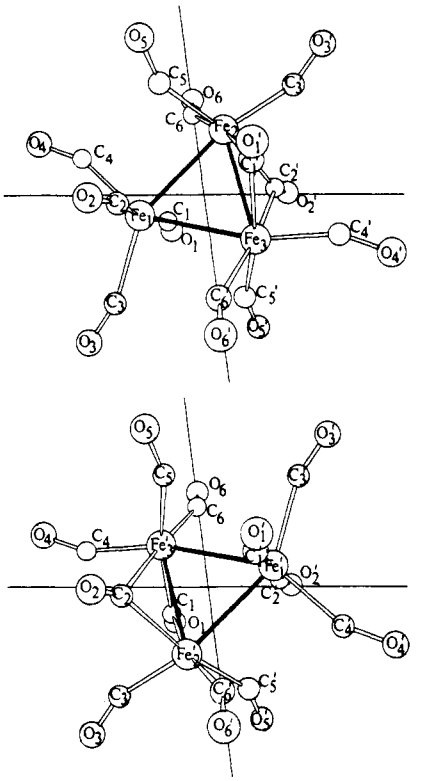

Figure 1. Molecular structure of $Fe_3(CO)_{12}$ showing the two orientations of the triangle of iron atoms within the carbonyl framework, which remains essentially unchanged. The structure is a random distribution of 50% of each orientation such that each iron site has an occupancy of 0.5.

were prepared by dispersing $Fe_3(CO)_{12}$ uniformly in Vaseline with a concentration of either 10 or 25 mg/cm² of sample. Different absorber thicknesses were used in order to avoid saturation effects at low temperature and to produce a significant percent effect at higher temperatures. This is illustrated in Figure 2, which shows the 295 K spectrum for both absorber concentrations. Virtually identical hyperfine parameters were obtained with either absorber at all temperatures studied. The 4.2 K Mössbauer spectrum was obtained in a different cryostat with a different geometry. This accounts for the smaller percent effect for this spectrum in Figure 2.

The asymmetry observed in the spectra at higher temperatures prompted us to investigate the presence of texture or crystallite orientation effects in our absorber. Absorbers prepared with extensive grinding and with grinding with both sugar and boron nitride gave results virtually identical with those discussed herein. As a further test for the presence of texture, a series of spectra were obtained at four different orientations of the sample mounted at the magic angle with respect to the Mössbauer γ-ray direction.[7] The results of these experiments are discussed in terms of a Goldanskii–Karyagin asymmetry. Unfortunately, we were unable to observe a frozen-solution Mössbauer spectrum with an unenriched

(2) Wei, C. H.; Dahl, L. F. *J. Am. Chem. Soc.* **1969**, *91*, 1351–1361.
(3) Cotton, F. A.; Troup, J. M. *J. Am. Chem. Soc.* **1974**, *96*, 4155–4159.
(4) Erickson, N. E.; Fairhall, A. W. *Inorg. Chem.* **1965**, *4*, 1320–1322.
(5) Dahl, L. F.; Blount, J. F. *Inorg. Chem.* **1965**, *4*, 1373–1375.
(6) Benson, C. G.; Long, G. J.; Kolis, J. W.; Shriver, D. F. *J. Am. Chem. Soc.* **1985**, *107*, 5297–5298.
(7) Greneche, J. M.; Varret, F. *J. Phys., Lett.* **1982**, *43*, L233–L237.

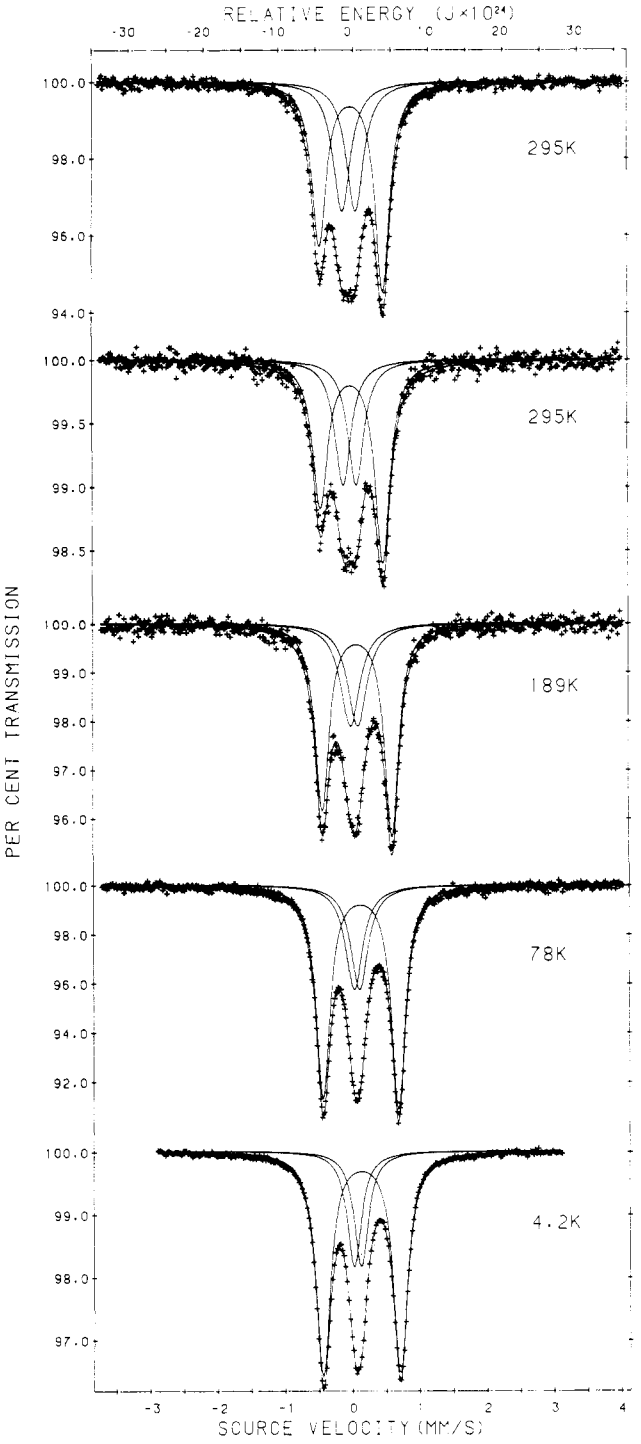

Figure 2. Mössbauer spectra of $Fe_3(CO)_{12}$ obtained at 295, 189, 78 and 4.2 K. The top spectrum absorber thickness was 25 mg/cm^2. For the remaining spectra the absorber thickness was 10 mg/cm^2.

sample dissolved in 50:50 acetone–water.

Results and Discussion

The Mössbauer spectra of $Fe_3(CO)_{12}$ obtained at 4.2, 78, 189, and 295 K are illustrated in Figure 2, and the spectral parameters are given in Table I. The solid lines in Figure 2 are the result of a least-squares fit with a quadrupole doublet for the outer lines, whose line widths are constrained to be equal, and a quadrupole doublet for the inner lines, whose line widths and areas are constrained to be equal; hence, nine parameters were adjusted. In this analysis, the outer doublet is assigned to the two equivalent iron atoms, Fe_B, in the C_{2v} structure, I, and the inner doublet is assigned to the unique iron atom, Fe_A.

As is apparent in Figure 2, changes occur in both the hyperfine parameters and in the relative areas of the two doublets with increasing temperature. Figure 3 shows the change, from 4.2 to 295 K, of the isomer shifts, δ_A and δ_B, the quadrupole splittings, $\Delta E_{Q,A}$ and $\Delta E_{Q,B}$, respectively, for the A and B iron sites in $Fe_3(CO)_{12}$, and the area ratios, A_B/A_A and A_1/A_4, where A_1 and A_4 are the areas of the low- and high-velocity components of the outer quadrupole doublet. Both isomer shifts, δ_A and δ_B, show a typical second-order Doppler shift with the slopes given in Table II. The 0.2 mm/s decrease in the quadrupole splitting, $\Delta E_{Q,B}$, between 4.2 and 295 K is not anomalous. The temperature dependence of the quadrupole splitting, $\Delta E_{Q,A}$, indicates that the quadrupole splitting for the Fe_A site is negative as shown in Figure 3. The alternative positive sign for $\Delta E_{Q,A}$ leads to an anomalous temperature dependence in which $\Delta E_{Q,A}$ increases with increasing temperature. An explanation for this unusual result is presented at the end of this section. The area ratio A_B/A_A is 1.90, or nearly 2 as expected, at 4.2 K, but decreases markedly with increasing temperature to reach a value of 1.27 at 295 K for a thin absorber. The area ratio A_1/A_4 is equal to 1, and the outer quadrupole doublet is symmetric at 4.2 K. However, with increasing temperature this ratio decreases to a value of 0.72 at 295 K for the 10 mg/cm^2 absorber, indicating an asymmetric doublet. The following sections will present an account of these features in terms of the Goldanskii–Karyagin effect, the relative recoil-free fractions of the two sites, and the different contributions to the quadrupole interaction.

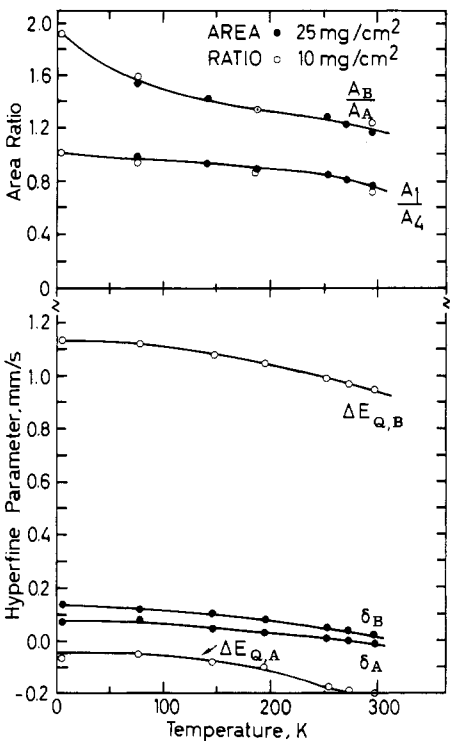

Figure 3. Temperature dependence of the Mössbauer effect hyperfine parameters and area ratios for $Fe_3(CO)_{12}$ obtained from fits with two quadrupole doublets.

Table II. Recoil-Free Fraction Determination for $Fe_3(CO)_{12}$

	Fe_A	Fe_B	av
$d\delta/dT$, (mm/s)/K	-4.10×10^{-4}	-5.15×10^{-4}	-4.62×10^{-4}
$d(\ln A)/dT$	-6.32×10^{-3}	-7.64×10^{-3}	-7.09×10^{-3}
M_{eff}[a]	102	81	90
θ_M,[b] K	110	112	110
f[c] at 300 K	0.14	0.09	0.11
f[c] at 200 K	0.27	0.20	0.23
f[d] at 100 K	0.32	0.26	0.28
f[e] at 300 K	0.12	0.09	

[a] Obtained from ref 18, eq 16. [b] Obtained from ref 18, eq 18. [c] Obtained from ref 18, eq 19. [d] Obtained from ref 18, eq 21. [e] Obtained from crystallographic data[3] as explained in the text and ref 17.

Perhaps the most surprising aspect of Figure 3 is the temperature dependence of both the area ratio for the two sites, A_B/A_A, and the area ratio of the two components of the outer quadrupole doublet, A_1/A_4. In the first case we would initially expect, on the basis of the structure, a value of 2 for A_B/A_A, independent of temperature. In the second case we would expect a value of 1 for A_1/A_4, also independent of temperature. Hence we must examine the reasons for the departure of these ratios from the expected values.

One possible explanation in both cases would be the presence of an impurity coincident with the higher velocity lines found in $Fe_3(CO)_{12}$. This impurity would have to have a quadrupole splitting of 0.5 mm/s and an isomer shift of 0.3 mm/s at room temperature and a recoil-free fraction quite different from that of $Fe_3(CO)_{12}$. This explanation seems very unlikely because repeated and different preparations of $Fe_3(CO)_{12}$ have led to exactly the same spectra. These preparations have included sublimation and recrystallization from different solvent mixtures of samples obtained from different sources. Further, the amount of impurity that would account for the A_1/A_4 value at room temperature cannot account for the small value of A_B/A_A at this temperature.

A crystallographic phase change upon cooling seems unlikely because the Mössbauer spectrum obtained at 4.2 K is in agreement with the structure observed at room temperature.[2,3]

Structural dynamic effects[8,9] on the Mössbauer time scale could be invoked to explain the variation in the A_B/A_A area ratio. We have examined in detail several dynamic models based upon both the solution[10-12] and solid-state[8,9] properties of $Fe_3(CO)_{12}$. Details of these models are presented in the Appendix. In no case were the models able to account for the observed spectral line shape. Hence, dynamic effects are not the explanation.

The low value of A_1/A_4 found at room temperature could result from texture[7] or preferential crystallite orientation in the Mössbauer absorber. In preparing a powder Mössbauer absorber, such a partial orientation is often obtained and manifests itself as a difference in the areas of the two components of the normally symmetric quadrupole doublet that would be obtained from a random powder.[13,14] The presence of such texture is possible for our absorbers, and consequently, we carried out several experiments to detect its presence. The spectra of two samples of different thicknesses, 10 and 25 mg/cm^2, showed little difference in the asymmetry of the outer lines (see Figure 3). This independence of sample thickness eliminates the possibility that the asymmetry could arise from line-shape effects.[13] Three room-temperature spectra were obtained with absorbers that contained 10 mg/cm^2 of $Fe_3(CO)_{12}$ which had been finely ground, finely ground with sugar, or finely ground with boron nitride. The resulting spectra were all virtually identical with that shown in Figure 2 and gave an A_1/A_4 ratio of 0.74 (2) in each case.

For unpolarized iron-57 Mössbauer spectroscopy, Greneche and Varret[7] have described a method that provides the equivalent of a random powder spectrum for any sample, with any hyperfine interactions. In this method, the normal to the absorber plane makes an angle, the so-called magic angle, of 54.7° with the Mössbauer γ-ray direction. Four spectra, obtained at the magic angle, but with the sample absorber plane rotated by 90° about its normal, i.e. at 0, 90, 180, and 270°, are measured and summed together. If any texture is present in the absorber, the four resulting spectra will have different quadrupole doublet component area ratios, but their sum will be symmetric.[7] Figure 4 shows the

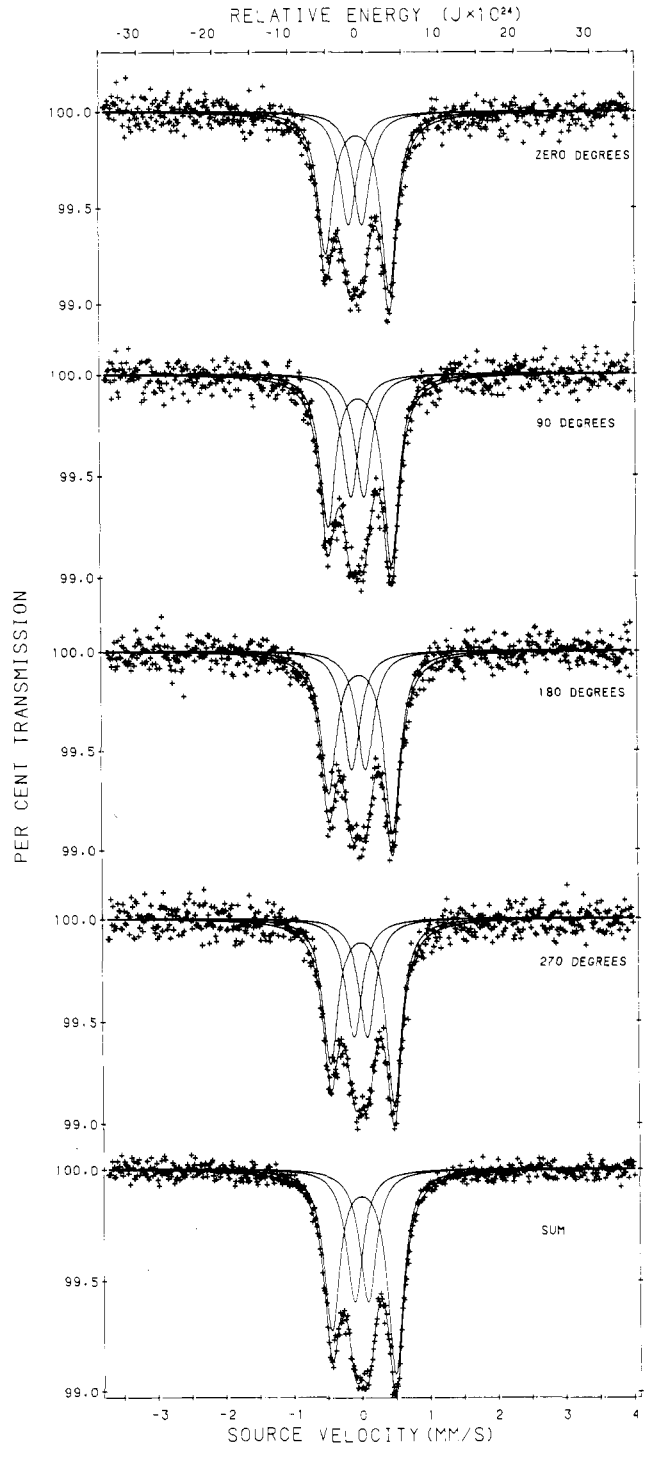

Figure 4. Room-temperature Mössbauer spectra of $Fe_3(CO)_{12}$ for four orientations of the sample all obtained at the magic angle (see text).

results obtained in such an experiment at room temperature for an absorber containing 10 mg/cm^2 of $Fe_3(CO)_{12}$. The statistics for these spectra are poorer than those observed in Figure 2 because of the thin absorber used in this case and because of the nonideal source–absorber–detector geometry required for the "magic-angle" experiment. However, it is apparent that each spectrum shows the same A_1/A_4 area ratio (the actual values are 0.78, 0.80, 0.77, and 0.78) and the summed spectrum has an area ratio of 0.78 for the outer doublet, a value which is in good agreement with the vertical absorber spectrum. Hence it is impossible that our absorbers contain any texture that could account for the area asymmetry in the outer quadrupole doublet. Furthermore, as discussed by Gibb et al.[13] and Chandra and Ericsson,[14] the asymmetry due to texture is independent of temperature, contrary to our observation.

(8) Dorn, H.; Hanson, B. E.; Motell, E. *Inorg. Chim. Acta* **1981**, *54*, L71–L73.
(9) Hanson, B. E.; Lisic, E. C.; Petty, J. T.; Iannaconne, G. A. *Inorg. Chem.* **1986**, *25*, 4062–4064.
(10) Cotton, F. A.; Hunter, D. L. *Inorg. Chim. Acta* **1974**, *11*, L9–L10.
(11) Johnson, B. F. G. *J. Chem. Soc., Chem. Commun.* **1976**, 703–704.
(12) Johnson, B. F. G.; Benfield, R. E. In *Transition Metal Clusters*; Johnson, B. F. G., Ed., Wiley: New York, **1980**; pp 471–543.
(13) Gibb, T. C.; Greatrex, R.; Greenwood, N. N. *J. Chem. Soc. A* **1968**, 890–894.
(14) Chandra, R.; Ericsson, T. *Hyperfine Interact.* **1979**, *7*, 229–239.

A final explanation for the area asymmetry in the outer quadrupole doublet is the Goldanskii–Karyagin effect.[15,16] In this case the asymmetry of the doublet is due to lattice vibrational anisotropy. The recoil-free fraction is a function of the mean square displacement of the iron-57 nucleus; therefore, if vibrational anisotropy is present, the recoil-free fraction will depend upon the orientation of a given crystallite. Thus, when averaging over all orientations for a powder, the intensity ratio for the two lines of a doublet is different from 1 and the resulting asymmetry increases as temperature increases as is observed in Figure 3. The Goldanskii–Karyagin effect is seldom observed in iron-57 Mössbauer spectra because the recoil-free fraction for iron-57 is often close to 1, as noted by Chandra and Ericsson,[14] who observed the presence of Goldanskii–Karyagin asymmetry in the spectra of $FePS_3$, a material that has a crystallographic structure favorable for high vibrational anisotropy and a low recoil-free fraction of 0.35.[17a] The crystallographic structure of $Fe_3(CO)_{12}$ is also favorable for vibrational anisotropy because of the planar arrangement of the three iron atoms. As shown by the thermal ellipsoids computed from the X-ray diffraction results, the iron vibrations are markedly anisotropic.[3] Following the approach of Spiering[17a] for an axial anisotropy in the case of Fe_A in $Fe_3(CO)_{12}$ and for a nonaxial anisotropy in the case of Fe_B, we can compute an average recoil-free fraction, or f factor, at room temperature of 0.12 for the A site iron nucleus and an average of 0.09 for each of the two B site iron nuclei. These small values of the recoil-free fractions are favorable for the observation of the Goldanskii–Karyagin effect.[14] From the crystallographic data we can calculate, as explained in ref 17b, for the A site, with $N = -0.72$, $\zeta_0^2 = 0.51$, and $A_{20}^{\pi} = 0.025$, a value of 0.90 for the area ratio of the inner doublet lines at room temperature and, for the B sites, with $N = 4.22$ (3.84), $n = 0.52$ (0.67), $\zeta_0^2 = -1.65$ (−1.62), and $A_{20}^{\pi} = -0.08$ (−0.08), a value of 0.72 for the area ratio of the outer doublet lines at room temperature. This latter number agrees very well with the area ratio of 0.72 observed at room temperature for the 10 mg/cm^2 sample and the values of 0.78 observed at room temperature for the 25 mg/cm^2 sample and the magic-angle spectrum. Because of the small quadrupole splitting of the inner doublet, it is not easy to detect any asymmetry in this spectral component. Thus, from the crystallographic data on $Fe_3(CO)_{12}$, we may compute a Goldanskii–Karyagin effect giving rise to a doublet asymmetry which is in good agreement with that observed at room temperature.

We still must account for the large decrease in A_B/A_A from the expected value of 2 with increasing temperature. This ratio can be given as

$$\frac{A_B}{A_A} = \frac{f_B N_B}{f_A N_A}$$

where f_A and f_B are the recoil-free fractions of the A and B sites and N_A and N_B are the number of iron atoms on the A and B sites and are 1 and 2, respectively, for $Fe_3(CO)_{12}$. A plot of the temperature dependence of the isomer shift and the natural logarithm of the absorption area for each of the iron sites in $Fe_3(CO)_{12}$ is linear and yields the slopes given in Table II. From these values it is possible to calculate[18] the effective mass of the Mössbauer nuclide, the Mössbauer lattice temperature, θ_M, and finally the recoil-free fraction for a Mössbauer nuclide. The resulting values for $Fe_3(CO)_{12}$ are also given in Table II. From these f factors it is then possible to calculate A_B/A_A, and we obtain a value of 1.29 at 295 K, a value in excellent agreement with the observed value of 1.27 in the thin absorber. At 100 K we calculate an A_B/A_A ratio of 1.63, which is slightly larger than the ca. 1.55 value observed. The f factors are small and make $Fe_3(CO)_{12}$ an excellent molecule in which to observe the Goldanskii–Karyagin effect. Furthermore, the f factors obtained from the Mössbauer spectral results agree well with those obtained from the crystallographic results (see Table II).

By using the recoil-free fractions obtained from the room-temperature crystallographic structure,[3] we obtain at room temperature a ratio of A_B/A_A of 1.5, a value that is slightly larger than the observed ratio of 1.27. Hence the observed ratio is smaller than the calculated value but is in good agreement, considering the approximations[17a] contained in the calculated value.

It should be noted that the Fe_A site, which has the smaller average bond length[3] of 1.68 Å, has the larger recoil-free fraction of 0.14. In contrast, the two Fe_B sites, which have the larger average bond length of 1.73 Å, if the Fe_B–Fe_B bond is included, or 1.81 Å, if it is not included, have the smaller recoil-free fraction of 0.09. As expected, the more confined iron site has the higher recoil-free fraction. Upon cooling, the Mössbauer spectra indicate that the two recoil-free fractions will approach each other and are essentially the same at 4.2 K.

It is well-known[19] that the temperature coefficient of the quadrupole interaction is negative, and this is the case for both sites in $Fe_3(CO)_{12}$ if ΔE_Q is positive for the B site and negative for the A site. This behavior may be accounted for in two ways. First we must consider both the lattice, q_{lat}, and valence, q_{val}, contributions to the electric field gradient at the iron sites. On the basis of the site symmetries[3] in $Fe_3(CO)_{12}$, we estimate that the lattice contribution, q_{lat}^A, at the A site is essentially zero and, at most, is slightly temperature dependent. In contrast, q_{lat}^B for the B site is large and positive and at most slightly temperature dependent. Normally, one might expect the valence contribution, q_{val}, to the electric field gradient to be zero in low-spin diamagnetic complexes of this type. However, recent calculations of Harris and Bradley[20] have shown, in the related organoiron butterfly clusters, that the iron atoms have partial occupancy of the 3d and 4p orbitals, which may produce a nonzero q_{val}. In order to account for the temperature dependence in ΔE_Q for the A site, q_{val}^A must be negative and a function of temperature. Apparently there is a change in the orbital populations with increasing temperature that makes q_{val} and hence the quadrupole interaction more negative. Such changes in the orbital populations with temperature may result from changes in the iron–iron and/or iron–carbon bond lengths or perhaps from changes in the rather unusual[3] iron–carbon–oxygen bond angles. On this bases we have assigned $\Delta E_{Q,A}$ a negative value in Table I and Figure 3. Alternatively, small changes in the molecular structure upon cooling may be sufficient to change the magnitude of $\Delta E_{Q,A}$ and yield the unusual temperature dependence. We are currently undertaking a low-temperature single-crystal X-ray study of $Fe_3(CO)_{12}$ to investigate this possibility. The low-temperature structure will also permit us to estimate the low-temperature recoil-free fractions.

It is interesting to note that the observed temperature dependences of the quadrupole interactions in $Fe_3(CO)_{12}$ are similar to those observed in metals.[19] These temperature dependences may be fit by the empirical expression

$$\Delta E_Q(T) = [\Delta E_Q(0)](1 - bT^{3/2})$$

where $\Delta E_{Q,A}(0)$ is −0.084 mm/s, b_A is 2.55×10^{-4}, $\Delta E_{Q,B}(0)$ is 1.146 mm/s, b_B is 3.30×10^{-5}. These b values are quite comparable to literature values.[19]

Acknowledgment. We thank Drs. S. Mørup, M. Thomas, C. E. Johnson, B. E. Hanson, D. Jones, F. E. Berry, and H. Kaesz for many helpful discussions during the course of this work and M. L. Buhl for experimental help. Further, we thank the donors of the Petroleum Research Fund, administered by the American Chemical Society, for their support of this research and NATO for a cooperative scientific research grant (No. 86/685). G.J.L. thanks the SERC of the U.K. for a faculty science research

(15) Goldanskii, V. I.; Gorodinskii, G. M.; Karyagin, S. V.; Korytko, L. A.; Kriyhanskii, L. M.; Markarov, E. F.; Suzdalev, I. P.; Khrapov, V. V. *Dokl. Phys. Chem. (Engl. Transl.)* **1963**, *147*, 766.
(16) Karyagin, S. V. *Dokl. Akad. Nauk SSSR* **1963**, *148*, 1102.
(17) Spiering, H. In *Mössbauer Spectroscopy Applied to Inorganic Chemistry*; Long, G. J., Ed., Plenum: New York, 1984; Vol. 1: (a) pp 77–170; (b) pp 129–131.
(18) Herber, R. H. In *Chemical Mössbauer Spectroscopy*; Herber, R. H., Ed., Plenum: New York, 1984; pp 199–216.
(19) Raghavan, R. S.; Kaufmann, E. N.; Raghavan, P. *Phys. Rev. Lett.* **1975**, *34*, 1280.
(20) Harris, S.; Bradley, J. S. *Organometallics* **1984**, *3*, 1086–1093.

fellowship at the University of Liverpool during 1983–1984.

Appendix

The fluxionality of $Fe_3(CO)_{12}$ (I) in the solid state is suggested by its solid-state carbon-13 NMR spectrum.[8] Dorn et al.[8] and Hanson et al.[9] assume a rapid motion of the molecule in agreement with the Star of David arrangement, II. They propose that the triangle of iron atoms rotates by 60° with a concomitant motion of 0.08 Å perpendicular to the plane for a total displacement[2] of ca. 1.5 Å for each of the three iron atoms. This motion takes the molecule from one orientation to the other orientation shown in Figure 1. The activation energy for this process is 41.8 kJ/mol,[9] a large but reasonable value for such a dramatic process.

We have modeled this 60° rotational process in an attempt to fit the Mössbauer spectra from 4.2 to 295 K. In this model each iron atom is relaxing between two states, i.e. site A and site B. Litterst and Amthauer[21] have studied in detail such relaxation, and in the case where the characteristic spectrum of each state is a doublet, the Mössbauer line shape is given by

$$\phi(x) = I\left\{\frac{(\Gamma/2 + 2(\lambda_- p_1^2 + \lambda_+ p_2^2))A - (x - p_1\epsilon_2 - p_2\epsilon_1)B}{A^2 + B^2} + \left[\frac{(\Gamma/2 + 2(\lambda_- p_1^2 + \lambda_+ p_2^2))A' - (x - p_1\epsilon_2' - p_2\epsilon_1')B'}{A'^2 + B'^2}\right]H\right\} \quad (1)$$

where I is the total spectral absorption area, x is the velocity, $\Gamma/2$ is the half-width at half-height of the Lorentzian absorption line in the absence of relaxation, p_1 and p_2 are the relative populations of states 1 and 2 respectively, λ_+ and λ_- are the relaxation rates from state 1 to state 2 and from state 2 to state 1 respectively, H is the ratio of the intensity of the two components of the doublet, and A, A', B, and B' are given by

$$A = (x - \epsilon_1)(x - \epsilon_2) - (\Gamma/2)(\Gamma/2 + (\lambda_+ p_2 + \lambda_- p_1))$$

$$A' = (x - \epsilon_1')(x - \epsilon_2') - (\Gamma/2)(\Gamma/2 + (\lambda_+ p_2 + \lambda_- p_1))$$

$$B = (\Gamma/2)(2x - \epsilon_1 - \epsilon_2) + \lambda_+ p_2(x - \epsilon_2) + \lambda_- p_1(x - \epsilon_1)$$

$$B' = (\Gamma/2)(2x - \epsilon_1' - \epsilon_2') + \lambda_+ p_2(x - \epsilon_2') + \lambda_- p_1(x - \epsilon_1')$$

with

$$\epsilon_1 = \delta_1 + {}^1/_4 e^2 q_1 Q \qquad \epsilon_1' = \delta_1 - {}^1/_4 e^2 q_1 Q$$

$$\epsilon_2 = \delta_2 + {}^1/_4 e^2 q_2 Q \qquad \epsilon_2' = \delta_2 - {}^1/_4 e^2 q_2 Q$$

where $\delta_{1/2}$ and $1/2e^2q_{1/2}Q$ are the isomer shift and the quadrupole splitting of state 1 or 2. The factor H is introduced to account for the Goldanskii–Karyagin asymmetry as discussed above. Indeed it was impossible to account for the asymmetry of the outer doublet with $H = 1$. It must be noted that the expressions given by Litterst and Amthauer[21] have been modified to introduce two relaxation rates, λ_+ and λ_-, which are necessary when the relative populations, p_1 and p_2, are different. Furthermore, λ_+, λ_-, p_1, and p_2 are related by the expressions[22] $\lambda_+ p_1 = \lambda_- p_2$, and $p_1 + p_2 = 1$. For the 60° rotational model, state 1 represents the A site and state 2 the B site. Each iron has a one-third probability of being on the unique A site in the C_{2v} structure and a two-thirds probability of being on the B site. Thus, in (1), $p_1 = {}^1/_3$, $p_2 = {}^2/_3$, and $\delta_{1/2}$ and $1/2e^2q_{1/2}Q$ are respectively $\delta_{A(B)}$ and $\Delta E_{Q,A(B)}$ for the two iron sites in the C_{2v} structure. This model is unable to account for the temperature dependence of A_B/A_A because, on average, it has an area ratio of 2 at all temperatures as a result of the fixed values of p_1 and p_2. We have also tried a slight variation in this model. It is possible that the probability of having the iron triangle in the two orientations shown in Figure 1 are different. However, even with this assumption, each iron atom has a probability of ${}^1/_3$ of being on the A site and ${}^2/_3$ of being on the B site. Consequently, this variation fails for the same reason the simpler model failed.

So far, (1) implicitly assumes that both sites A and B have the same recoil-free fractions, but as discussed above, we know that this is not the case. Thus, in order to represent the difference in the recoil free fractions, the populations p_1 and p_2 were allowed to depart from ${}^1/_3$ and ${}^2/_3$. The resulting fits are rather satisfactory but show systematic deviations from the experimental data and are poorer than those shown in Figure 2. Furthermore, the relaxation rate, λ_+, is very small at all temperatures and shows random variation with temperature. In conclusion, the 60° rotational model does not account for the Mössbauer spectra, which, in fact, show narrow line widths (see Table I). Thus, the 60° rotation process, which is observed by carbon-13 NMR, is not seen in the Mössbauer spectra. This can be understood in terms of the characteristic time scale of each technique.

The NMR time scale is typically in the range of 10^{-2} to 10^{-6} s, and for $Fe_3(CO)_{12}$, Hanson[23] computes an exchange lifetime of 8×10^{-4} s or a relaxation rate of 1.25×10^3 s^{-1} at 295 K. The Mössbauer time scale is given by the lifetime of the excited level of iron-57, 97.8×10^{-9} s, or a corresponding frequency of 1.02×10^7 s^{-1}. Thus, the motion observed in the NMR spectra has a lifetime much longer than the Mössbauer effect characteristic time. For Mössbauer spectroscopy, the situation is equivalent to a static configuration, and the spectrum is only the superposition of the doublets characteristic of the A and B sites as shown in the fits of Figure 2.

The fluxionality of $Fe_3(CO)_{12}$ in solution has been extensively studied. A possible mechanism involving carbonyl scrambling has been proposed by Cotton and Hunter,[10] and a mechanism for carbonyl migration has been proposed by Johnson.[11] The first step in the migration mechanism takes the molecule from the C_{2v} structure, observed in the solid state, to the D_3 structure.[11] This D_3 structure is obtained by rotation of the iron triangle by 30° about its C_2 axis. The carbonyl framework remains nearly fixed during this rotation. In the D_3 structure, all carbonyl ligands are terminal and equivalent and all iron–iron distances are equal. It is interesting to note that this rocking motion of the iron triangle implies a displacement of only two of the three iron atoms of ca. 0.6 Å. This molecular rearrangement is much less dramatic than the one considered by Dorn et al.[8] in the solid state. Thus, one would expect a mechanism such as that described by Johnson[11] to be possible in the solid state.

In order to represent the C_{2v} to D_3 relaxation, we must superimpose two profiles as given by (1) with relative intensities of 1:2. One profile represents one iron atom relaxing between state 1, Fe_A, and state 2, Fe_D, in the D_3 structure whereas the second profile represents two iron atoms relaxing between state 1, Fe_B, and state 2, Fe_D. Thus for the first profile, we have

$$\epsilon_1 = \delta_A + {}^1/_2\Delta E_{Q,A} \qquad \epsilon_1' = \delta_A - {}^1/_2\Delta E_{Q,A'}$$

and for the second profile

$$\epsilon_1 = \delta_B + {}^1/_2\Delta E_{Q,B} \qquad \epsilon_1' = \delta_B - {}^1/_2\Delta E_{Q,B'}$$

where $\delta_{A(B)}$ and $\Delta E_{Q,A(B)}$ are the isomer shift and quadrupole splitting for Fe_A or Fe_B. For both profiles we have

$$\epsilon_2 = \delta_D + {}^1/_2\Delta E_{Q,D} \qquad \epsilon_2' = \delta_D - {}^1/_2\Delta E_{Q,D'}$$

where δ_D and $\Delta E_{Q,D}$ are the isomer shift and quadrupole splitting for Fe_D.

Fits were obtained by making several assumptions that we do not need to detail here, which reduce the number of parameters from 12 to six. The fits show systematic deviations from the experimental data especially in the central part of the spectra and for temperatures above 188 K. Therefore, we conclude that this rocking model is not observed in the solid-state Mössbauer spectrum of $Fe_3(CO)_{12}$.

Registry No. $Fe_3(CO)_{12}$, 17685-52-8.

(21) Litterst, F. J.; Amthauer, G. *Phys. Chem. Miner.* **1984**, *10*, 250–255.
(22) Prietsch, M.; Wortmann, G.; Kaindl, G.; Schlöyl, R. *Phys. Rev. B.: Condens. Matter* **1986**, *33*, 7451.
(23) Hanson, B. E., private communication.